RESEARCH ARTICLE

Cortical Network Dysfunction Caused by a Subtle Defect of Myelination

Giulia Poggi,[1] Susann Boretius,[2,3] Wiebke Möbius,[4] Nicole Moschny,[1] Jürgen Baudewig,[2,3] Torben Ruhwedel,[4] Imam Hassouna,[1] Georg L. Wieser,[4] Hauke B. Werner,[4] Sandra Goebbels,[4] Klaus-Armin Nave,[4,5] and Hannelore Ehrenreich[1,5]

Subtle white matter abnormalities have emerged as a hallmark of brain alterations in magnetic resonance imaging or upon autopsy of mentally ill subjects. However, it is unknown whether such reduction of white matter and myelin contributes to any disease-relevant phenotype or simply constitutes an epiphenomenon, possibly even treatment-related. Here, we have re-analyzed *Mbp* heterozygous mice, the unaffected parental strain of *shiverer*, a classical neurological mutant. Between 2 and 20 months of age, $Mbp^{+/-}$ versus $Mbp^{+/+}$ littermates were deeply phenotyped by combining extensive behavioral/cognitive testing with MRI, 1H-MR spectroscopy, electron microscopy, and molecular techniques. Surprisingly, Mbp-dependent myelination was significantly reduced in the prefrontal cortex. We also noticed a mild but progressive hypomyelination of the prefrontal corpus callosum and low-grade inflammation. While most behavioral functions were preserved, $Mbp^{+/-}$ mice exhibited defects of sensorimotor gating, as evidenced by reduced prepulse-inhibition, and a late-onset catatonia phenotype. Thus, subtle but primary abnormalities of CNS myelin can be the cause of a persistent cortical network dysfunction including catatonia, features typical of neuropsychiatric conditions.

GLIA 2016;00:000–000

Key words: myelin basic protein (Mbp) mutant, Cnp mutant, prepulse inhibition, catatonia, MRI, electron microscopy

Introduction

The expansion of white matter tracts is among the most striking features of mammalian brain evolution and long-range connectivity along myelinated tracts is thought to underlie many aspects of higher brain function (Fields et al., 2014; Nave, 2010; Zatorre et al., 2012). The role of myelin for motor-sensory functions is well recognized, and illustrated by the grave neurological symptoms in patients with severe myelin abnormalities, such as leukodystrophies. In contrast, a potential impact of mildly disturbed myelination in psychiatric diseases is poorly understood. It is unknown, whether subtle alterations in myelin thickness or the number of myelinated axons in cortex and subcortical white matter tracts compromise higher brain functions. Theoretically, such subtle alterations could perturb the millisecond precision crucial for signal propagation in higher brain networks (Uhlhaas and Singer 2012), thereby explaining the often postulated "disconnectivity" syndromes (Catani and Ffytche, 2005; Schmahmann et al., 2008). Psychiatric symptoms have been documented in white matter defects, such as metachromatic leukodystrophy (Hyde et al., 1992) and multiple sclerosis (Feinstein et al., 2014). However, the role of oligodendrocyte and myelin defects in higher brain functions and diseases such as schizophrenia is largely unclear (Takahashi et al., 2011).

Myelin is made by oligodendrocytes as a multilayered membrane sheath and enables rapid axonal impulse propagation (Nave, 2010). Myelin membranes have a unique composition of lipids and proteins, including abundant structural

View this article online at wileyonlinelibrary.com. DOI: 10.1002/glia.23039

Published online Month 00, 2016 in Wiley Online Library (wileyonlinelibrary.com). Received Apr 26, 2016, Accepted for publication July 8, 2016.

Address correspondence to Hannelore Ehrenreich, Clinical Neuroscience, Max Planck Institute of Experimental Medicine, Hermann-Rein-Str.3, 37075 Göttingen, Germany. E-mail: ehrenreich@em.mpg.de and Klaus-Armin Nave, Neurogenetics, Max Planck Institute of Experimental Medicine, Hermann-Rein-Straße 3, 37075 Göttingen, Germany. E-mail: nave@em.mpg.de

From [1]Clinical Neuroscience, Max Planck Institute of Experimental Medicine, Göttingen; [2]Department of Radiology and Neuroradiology, Christian-Albrechts-University, Kiel; [3]Department of Functional Imaging, German Primate Center, Leibniz Institute of Primate Research, Göttingen; [4]Neurogenetics, Max Planck Institute of Experimental Medicine, Göttingen; [5]DFG Research Center for Nanoscale Microscopy and Molecular Physiology of the Brain (CNMPB), Göttingen, Germany

Imam Hassouna is on leave of absence from Physiology Unit, Zoology Department, Faculty of Science, Menoufia University, Shebin Elkom, Egypt

Additional Supporting Information may be found in the online version of this article.

components of CNS myelin, such as myelin basic protein (MBP), proteolipid protein (PLP), and cyclic nucleotide phosphodiesterase (CNP). MBP is important for myelin membrane compaction and therefore also essential in initiating and driving the axonal wrapping process (Jahn et al., 2009).

While myelination takes place largely during early postnatal life, there is continuous myelin growth in specific cortical areas, such as prefrontal cortex (PFC), lasting well into adult life (Miller et al., 2012). Recently, it has been shown that these sparsely myelinated areas regulate myelin growth differently than robustly myelinated subcortical regions, with neuronal activity and social interactions becoming a driving force of PFC development including its underlying white matter (Benes, 1989; Gibson et al., 2014; Liu et al., 2012; Makinodan et al., 2012; Tomassy et al., 2014; Uda et al., 2015).

Numerous reports have highlighted white matter abnormalities in psychiatric patients. This comprises findings by magnetic resonance imaging (MRI) of reduced white matter size and accelerated white matter aging (Balevich et al., 2015; Kochunov et al., 2013). Moreover, diffusion tensor imaging (DTI) and magnetic transfer resonance (MTR) have revealed abnormal connectivity and loss of white matter integrity in the corpus callosum of schizophrenia and bipolar patients (Balevich et al., 2015; Kubicki et al., 2005; Kubicki et al., 2002; McIntosh et al., 2008). Increased numbers of microglia in the proximity of myelinated fibers, suggesting neuroinflammation (Uranova et al., 2011), and reduced density of oligodendrocytes in PFC were reported in schizophrenia, bipolar disorder and major depression (Uranova et al., 2004).

Human autopsy material repeatedly revealed a decrease of several structural myelin proteins, such as MBP, and respective mRNAs (Chambers and Perrone-Bizzozero, 2004; Dracheva et al., 2006; Flynn et al., 2003; Hakak et al., 2001; Honer et al., 1999; Matthews et al., 2012; Parlapani et al., 2009; Tkachev et al., 2003). These correlative observations were made decades after disease onset. We also note that long-term antipsychotic medication is suspected to cause brain atrophy (Bartzokis et al., 2007; Ho et al., 2011) which includes myelinated fiber loss, and that pharmacological models of schizophrenia can trigger secondary myelin deficits (Zhang et al., 2012). Thus, distinguishing cause and consequence of myelin abnormalities in psychiatric disease has remained difficult. Whether mild changes of CNS myelination (in absence of overt neurological disease) affect cortical network functions can theoretically be addressed in animal models. Importantly, hypomyelination in these models must be subtle and not interfere with basic behavior if a causal impact on altered higher brain function shall be established.

Here, we studied mice heterozygous for the oligodendroglial *Mbp* gene, i.e., the healthy-appearing parents of dysmyelinated homozygous *Shiverer* mice (Chernoff, 1981; Readhead et al., 1987; Roach et al., 1985; Shine et al., 1992). We report a very subtle hypomyelination phenotype in $Mbp^{+/-}$ mice, which is more pronounced in the PFC than in caudal white matter tracts and progresses over time. Importantly, both basic behavior and cognition were normal, but we demonstrate a persistent defect of prepulse inhibition of the startle response (PPI), a surrogate marker for gating defects in human patients with schizophrenia and their first-degree relatives (Braff et al., 1978; Kumari et al., 2005). Moreover, we find late-onset catatonia and signs of low-grade inflammation. Our data in mice show that minor myelin abnormalities can be causal of cortical network dysfunctions, in the absence of other behavioral defects. These abnormalities alone can explain some of the pivotal phenotypes common to mental diseases.

Materials and Methods

Important Note

All experiments were performed by investigators unaware of group assignment ("fully blinded").

Mice

Experiments were approved by the local animal care and use committee. Mice were group-housed in standard plastic cages with access to food/water ad libitum, 12 h light-dark-cycle (light-on at 7:00 am), 20 − 22°C. Male $Mbp^{+/-}$ versus $Mbp^{+/+}$ mice [C57BL/6N background; genotyped as previously described (Klugmann et al., 1997)], and for comparator experiments, $Cnp^{+/-}$ versus $Cnp^{+/+}$ mice (Hagemeyer et al., 2012), were used.

Behavioral Testing

Male $Mbp^{+/-}$ versus $Mbp^{+/+}$ mice (littermates) underwent behavioral testing at 2 age-periods: 3 − 6 and 17 − 18 months. Experiments were conducted during light phase (9:00 − 17:00) in following order: Elevated plus maze, open field, hole board, prepulse inhibition of the startle response (PPI), rotarod, acoustic startle assessment, grip-strength, hot-plate, marble burying, olfaction (buried-food-test), visual-cliff, LABORAS home-cage observation, social interaction, Y-maze, sucrose preference, Morris water maze, and novel object recognition. Inter-test interval was $\geq$24 h. All tests were conducted as published in detail (Bodda et al., 2013; Dere et al., 2014; El-Kordi et al., 2013; Moy et al., 2004; Radyushkin et al., 2010). Tests yielding significance are described below.

Prepulse Inhibition of the Acoustic Startle Reflex (PPI), Testing Sensorimotor Gating

Mice are put in metal cages (82x40x40mm, restricting major movements), placed in sound-attenuating cabinets. Cages are equipped with a movable platform-floor attached to a sensor, recording vertical movements (TSE-Systems). Startle reflexes are evoked by acoustic stimuli delivered by a loudspeaker above the cage, connected to an

acoustic generator. The startle reaction to an acoustic stimulus inducing a movement of the force-sensitive platform is recorded over 260 ms beginning with pulse onset. An experimental session consists of 2-min habituation to a 65dB continuous background white noise, followed by 1 min baseline recording. Then, 6 pulse-alone trials (120 dB, 40 ms) are applied to decrease within-session habituation (not included in 120 dB/40 ms PPI analysis. For PPI, the startle pulse is applied either alone or preceded by a prepulse stimulus of 20-ms duration and 70-, 75-, or 80 dB intensity. A delay of 100 ms with background noise is interposed between prepulse and pulse. Trials are presented in pseudorandom order with variable intervals ranging from 8 to 22 s. The amplitude of the startle response (arbitrary units) is defined as the difference between the maximum force detected during the recording window and that measured immediately before stimulus onset. For each animal, amplitudes are averaged separately for trials with stimulus alone or stimulus preceded by prepulse. PPI is calculated as percentage of startle response using following formula: %PPI = 100-[(startle amplitude after prepulse)/(startle amplitude after pulse only)×100].

Startle Response to 120dB

Response to startle stimulus of 120dB alone, without any prepulse, and response without stimulus are recorded. The plain startle reaction to an acoustic pulse is a short-latency reflex mediated by an oligosynaptic neural circuit that includes lower brainstem, spinal and cranial motor neurons, and cerebellum (Kim et al., 2010; Takeuchi et al., 2001).

Bar Test for Catatonia

This test was performed as described (Hagemeyer et al., 2012; Kuschinsky and Hornykiewicz, 1972) and is illustrated in Supporting Information videos.

MRI And 1H-MR Spectroscopy (1H-MRS)

Mice were anesthetized with 5% isoflurane, intubated and kept under 1.75% isoflurane and 5% oxygen by active ventilation with constant respiratory frequency of 85 breaths/min (Animal-Respirator-Advanced^{TM}, TSE-Systems). MRI and 1H-MR spectroscopy (MRS) were performed at a magnetic field strength of 7T (ClinScan, Bruker-BioSpin). MRI comprised T2-weighted images (2D-FSE, TR/TE = 4000/50ms), diffusion-weighted images (2D-EPI, TR/TE= 7000/28 ms, 12 directions, $b = 0/1000 s/mm^2$) and 3 differently weighted 3D FLASH based datasets (TR/TE = 28/1.9 ms, flip-angle = 25° for T1-weighting and 5° for proton-weighting, the later with/without additional magnetization-transfer weighting by Gaussian-shaped off-resonance pulses with a flip-angle of 500° and an off-resonance frequency of 1200 Hz). Localized proton MR spectra (PRESS, TR/TE= 6000/10 ms) were obtained from a volume-of-interest in hippocampus ($1.8x0.7x1.8mm^3$), cortex ($3.9x0.7x3.2\ mm^3$) and corpus callosum ($3.9x0.7x1.7\ mm^3$). Metabolite quantification involved spectral evaluation by LCModel (Version 6.3-0G (Provencher, 1993)). Results with Cramer-Rao lower bounds >20% were excluded from further analyses. Maps of magnetization transfer ratio (MTR), magnetization saturation (MT_{SAT}), and diffusion tensor imaging (DTI) readouts, fractional anisotropy (FA), apparent diffusion coefficient (ADC), axial diffusivity (AD), and radial diffusivity (RD) were calculated using in-house Matlab scripts (Mathworks).

Electron Microscopy (EM)

Anesthetized mice were perfused intracardially with 15 mL HBSS, followed by 50 mL fixative (2.5% glutaraldehyde, 4% paraformaldehyde in phosphate buffer with 0.5% NaCl). Brains were dissected and 200 μm sagittal sections cut using Leica-VT1200S Vibratom (Leica-Microsystems). The genu of the corpus callosum was punched out of the sliced tissue, post-fixed with 2% OsO_4 (Science Services), dehydrated with ethanol/propylene oxide and Epon-embedded (Serva). Semi-thin sections were stained with methylene blue and AzurII. Ultrathin sections were contrasted with 4% uranyl acetate and lead citrate, scanned via Zeiss EM900 (Zeiss) and digital pictures obtained by wide-angle dual speed 2K-CCD-Camera (TRS). Myelin/axon tracings were performed on EM pictures (≥15/animal) via ImageJ (http://rsb.info.nih.gov/ij/). As myelin thickness index and inner tongue ratio, *g*-ratio and *t*-ratio were calculated.

Reverse Transcription and Real-Time PCR

For RNA analysis (PFC/brainstem), tissues were homogenized in Qiazol, chloroform added, samples centrifuged at 12,000*g*, 15 min, 4°C, extractions performed with miRNeasy mini-kit (QIAGEN), RNA concentration measured via absorbance at OD260nm and purity controlled (OD260/OD280). RNA (200 ng) was mixed with 0.6 pmol oligo dT-mix, 120 pmol of Random-Hexamer (Roche) and retro-transcribed to cDNA with SuperScript®III Reverse-Transcriptase-Kit (Life-Technologies). Derived cDNA (8 ng) was used as template for SYBR GREEN-based real-time PCR in Roche LightCycler 480. Samples were assayed in triplicate. Myelin mRNAs were normalized to 18s rRNA, microglia markers to the geometric mean of *Gapdh, β-Actin, Pbdg*. Following primers were used:

Mbp F5′-ACGGACACCCTTCCAAGTT-3′ R5′-GTGTGCCTCACCGTGAAAA-3′,

Cnp F5′-TAACCCTCCCTTAGCCCCTG-3′ R5′-GTCCCTAGCATGTGGCAGCT-3′,

Plp F5′-GGCTAGGACATCCCGACAAG-3′ R5′-GCAAACACCAGGAGCCATACA-3′,

18s F5′-GCTCTAGAATTACCACAGTTATCCAA-3′ R5′-AAATCAGTTATGGTTCCTTTGGTC-3′

iNos F5′-GGGCTGTCACGGAGATCA-3′ R5′-CCATGATGGTCACATTCTGC-3′

Tnfα F5'-GCCAACATCCCTACCTCTCC-3' R5'-CCCCAGGGCAAAGGTAAT-3'

*Arginase*1 F5′-AAGGAAAGTTCCCAGATGTACC-3′ R5′-GCAAGCCAATGTACACGATG-3′

β-Actin F5'-CTTCCTCCCTGGAGAAGAGC-3'R5′-ATGCCACAGGATTCCATACC-3′

Gapdh F5′-CAATGAATACGGCTACAGCAAC-3′ R5′-TTACTCCTTGGAGGCCATGT-3′

Pbdg F5′-ACAAGATTCTTGATACTGCACTCTCTAAG-3' R5′-CCTTCAGGGAGTGAACAACCA-3′

Western Blotting

Tissue was homogenized in lysis buffer (50 mM Tris/Cl pH7.5, 150 mM NaCl, 1 mM EDTA, 1% Triton x-100, 0.5% sodium deoxycholate) with addition of freshly prepared protease inhibitors (50 μg/mL Leupeptin, 0.2 mM phenylmethanesulfonylfluoride, 1 mM of activated sodium orthovandate, 30 μg/mL Aprotinin), incubated on ice (30 min) and centrifuged at 9000 rpm, 4°C, 10 min. After determination of protein concentration (Lowry et al., 1951), samples were mixed with 4X Lämmli-buffer and incubated at room temperature (30 min). Comparable amounts of total protein/sample were separated on 15% SDS polyacrylamide gels and transferred onto nitrocellulose. Membranes were blocked for ≥1 h at room temperature (Tris-buffered saline, 1% Tween, 5% powder milk) and incubated overnight at 4°C with primary antibody: anti-MBP (1:2,000, Dako), anti-CNPase (1:5,000, Sigma-Aldrich), anti-PLP (1 : 500, A431, produced in-house (Jung et al., 1996) and anti-α-Tubulin (1:10,000, Sigma-Aldrich). Incubation with secondary antibody, anti-mouse or anti-rabbit (1:5000, Rockland) followed for 2 h at room temperature. Bands were detected with Odyssey Infrared Imaging system and quantified via Image-Studio-Lite software. Intensities of Mbp, Cnp and Plp were normalized to α-Tubulin.

Immunohistochemistry

Anaesthetized mice were perfused with 4% paraformaldehyde (PFA), brains stored at −80°C. Coronal sections (30 μm) were immunolabeled for microglia marker anti-Iba1 (ionized calcium-binding adapter molecule 1; Wako, 1:1000 in 3% normal horse serum/0.5% TritonX-100), followed by donkey anti-rabbit antibody (R&D System, 594nm). Cell nuclei were counterstained with DAPI (4′,6-diamidino-2-phenylindole 1:10000, Sigma-Aldrich). Brain slices were scanned with inverted epifluorescence microscope (LEICA, DMI 6000B) and analyses performed with IMARIS software (http://www.bitplane.com/) and Fiji (http://fiji.sc/Fiji).

Statistical Analysis

Between-group comparisons were performed using t-test for independent samples and 2-way analysis of variance (ANOVA or repeated-measures ANOVA). Mann-Whitney U and Wilcoxon tests were applied when normality assumption was violated (Kolmogorov-Smirnov test). All statistics were performed using Prism GraphPad software or MatLab scripts (Mathworks). Data are expressed as mean ± SEM, P values <0.05 considered significant.

Results

Heterozygous $Mbp^{+/-}$ mice were long-lived, of normal body size, and without obvious abnormalities, including cage behavior and litter sizes, in agreement with classical studies of *Shiverer* ($Mbp^{-/-}$) mice (Chernoff, 1981; Readhead et al., 1987; Roach et al., 1985; Shine et al., 1992). At much lower level of *Mbp* expression (in partly complemented *Mbp*-transgenic *Shiverer* mice) Mbp is rate-limiting for myelination (Readhead et al., 1987). Thus, we hypothesized that also $Mbp^{+/-}$ mice might exhibit subtle defects of white matter formation, previously overlooked.

Spatio-Temporal Differences of Myelin Gene Expression

We quantified steady-state mRNA levels for the major myelin-specific proteins in PFC and brainstem (Fig. 1A–C). *Plp1* and *Cnp* mRNA, taken as indicator of oligodendrocyte number and differentiation, did not reveal any appreciable difference between $Mbp^{+/-}$ and $Mbp^{+/+}$ mice. Since oligodendrocytes do not die in *Shiverer* mice (Bu et al., 2004; Rosenbluth, 1980), *Plp1* and *Cnp* mRNA data confirmed that oligodendrocyte numbers are unchanged in aged $Mbp^{+/-}$ mice. In agreement with decreased *Mbp* gene dosage, *Mbp* mRNA was reduced by about 50% in $Mbp^{+/-}$ mice throughout postnatal development. Interestingly, at 20 months, this difference vanished (significance lost), both in PFC and brainstem (Fig. 1A). Thus, at older age, *Mbp* gene dosage appears no longer rate-limiting for *Mbp* mRNA abundance.

Mbp protein was reduced in tissue lysates by 50% in 3- and 6-month-old $Mbp^{+/-}$ mice, confirming previous studies (Barbarese et al., 1983). Plp/Dm20 and Cnp (normalized to α-tubulin) were not different in $Mbp^{+/-}$ mice, in line with mRNA data. However, in older mice (20 months), the Mbp content began to differ between brain regions. In the PFC, $Mbp^{+/-}$ mice expressed <25% of Mbp compared to $Mbp^{+/+}$, accompanied by a reduction of CNP by about 50%. In contrast, no further Mbp decrease was detected in brainstem (Fig. 1A–C). By EM, CNS myelin was well compacted and without obvious pathology (example in Fig. 2).

Subtle White Matter Defects Revealed by MRI And ^{1}H-NMR Spectroscopy

The qualitative inspection of T2-weighted MR images revealed minor thinning of the corpus callosum in 6 and 18 month-old $Mbp^{+/-}$ compared to $Mbp^{+/+}$ mice, associated with general mild reduction of white to grey matter contrast (Fig. 2A). Volume decrease together with 4% reduction of MTR indicates lower myelin content per pixel in $Mbp^{+/-}$ mice. This difference in MTR becomes even more evident when considering the observed 10% increase in T1 relaxation time. Due to the known dependence of MTR from T1 (Henkelman et al., 2001), this corresponds to a reduction of MT_{SAT} by 20% in the corpus callosum of $Mbp^{+/-}$ mice, both at 6 and 18 months (Fig. 2B, Table 1). MT_{SAT} increased with age, independent of genotype. Microstructural changes in neuronal fibers were analyzed by DTI. Upon aging, DTI of the corpus callosum revealed mild increase in FA in combination with minor decrease of AD, RD, and ADC (Table 1). However, all these changes were not *Mbp* genotype-dependent.

By 1H-MRS, reduced *Mbp* gene dosage had a small but (nominally) significant impact on brain metabolism. Most pronounced at 18 months, we noted increases in *myo*-inositol,

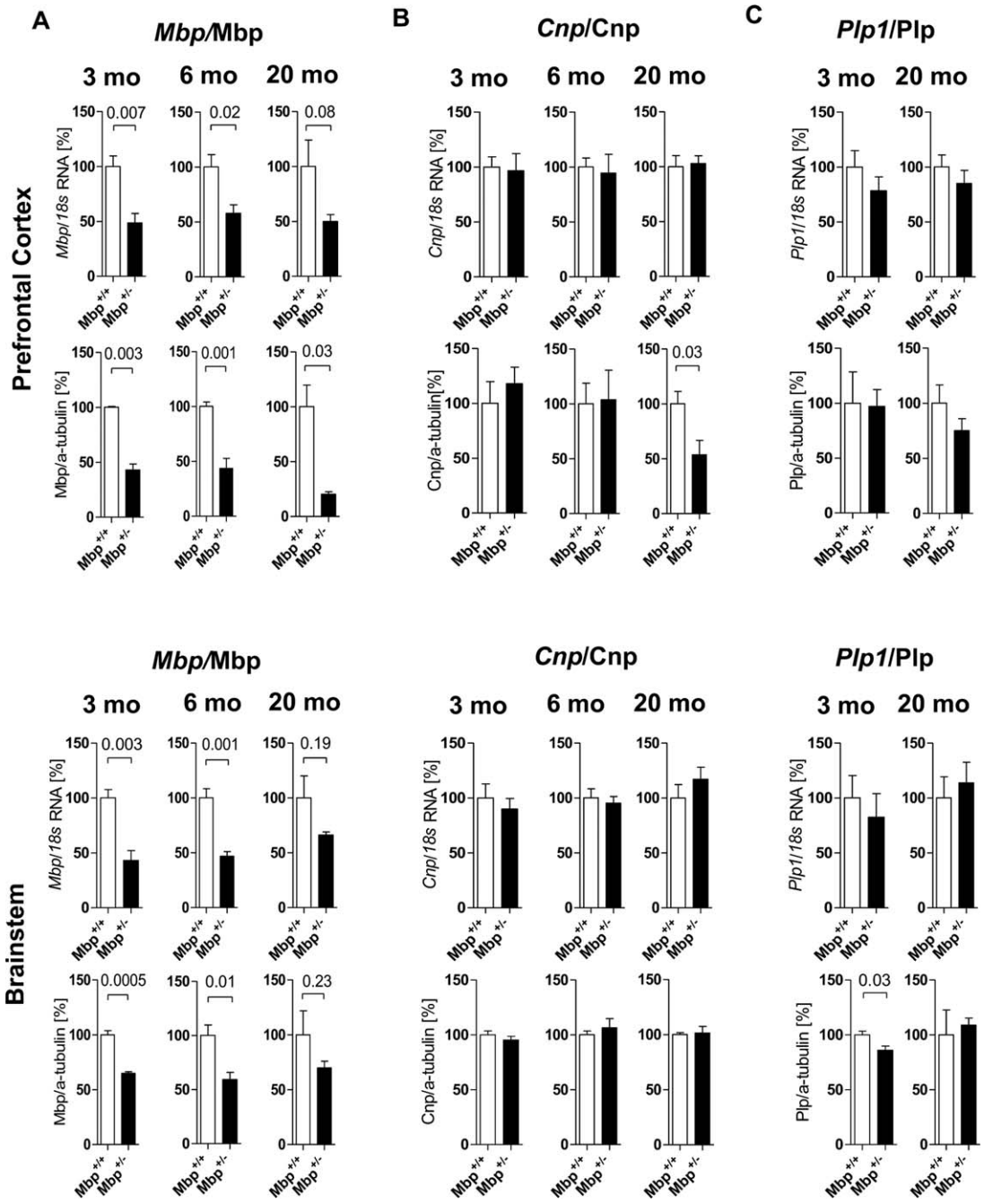

FIGURE 1: Myelin gene expression (mRNA, protein) in prefrontal cortex and brainstem of *Mbp*$^{+/-}$ versus *Mbp*$^{+/+}$ mice at 3 different ages. A: *Mbp*/Mbp, B: *Cnp*/Cnp, C: *Plp*/Plp. N = 4 per group; 2-sided t-tests, mean ± SEM presented.

taurine and total creatine in cortex and corpus callosum of *Mbp*$^{+/-}$ compared to *Mbp*$^{+/+}$ mice (Table 2). Since we found no difference for the neuronal marker NAA, and an increase in taurine (a potential neuroprotective agent (El Idrissi and Trenkner 1999)), *myo*-inositol elevation likely reflects age-dependent microglial activation in *Mbp*$^{+/-}$ mice (Badar-Goffer et al., 1992; Ross et al., 1997), and also total creatine would support glial changes (Urenjak et al., 1993).

Ultrastructure of CNS Myelin

To assess morphological correlates of reduced *Mbp* expression at the EM level, we analyzed the rostral corpus callosum in 18 month-old mice (Fig. 2C). Myelinated axons in cross-sections showed regularly compacted sheaths and no genotype-related pathology. Quantification revealed (as expected for EM micrographs) significant heterogeneity between subregions. This could explain why the percentage of

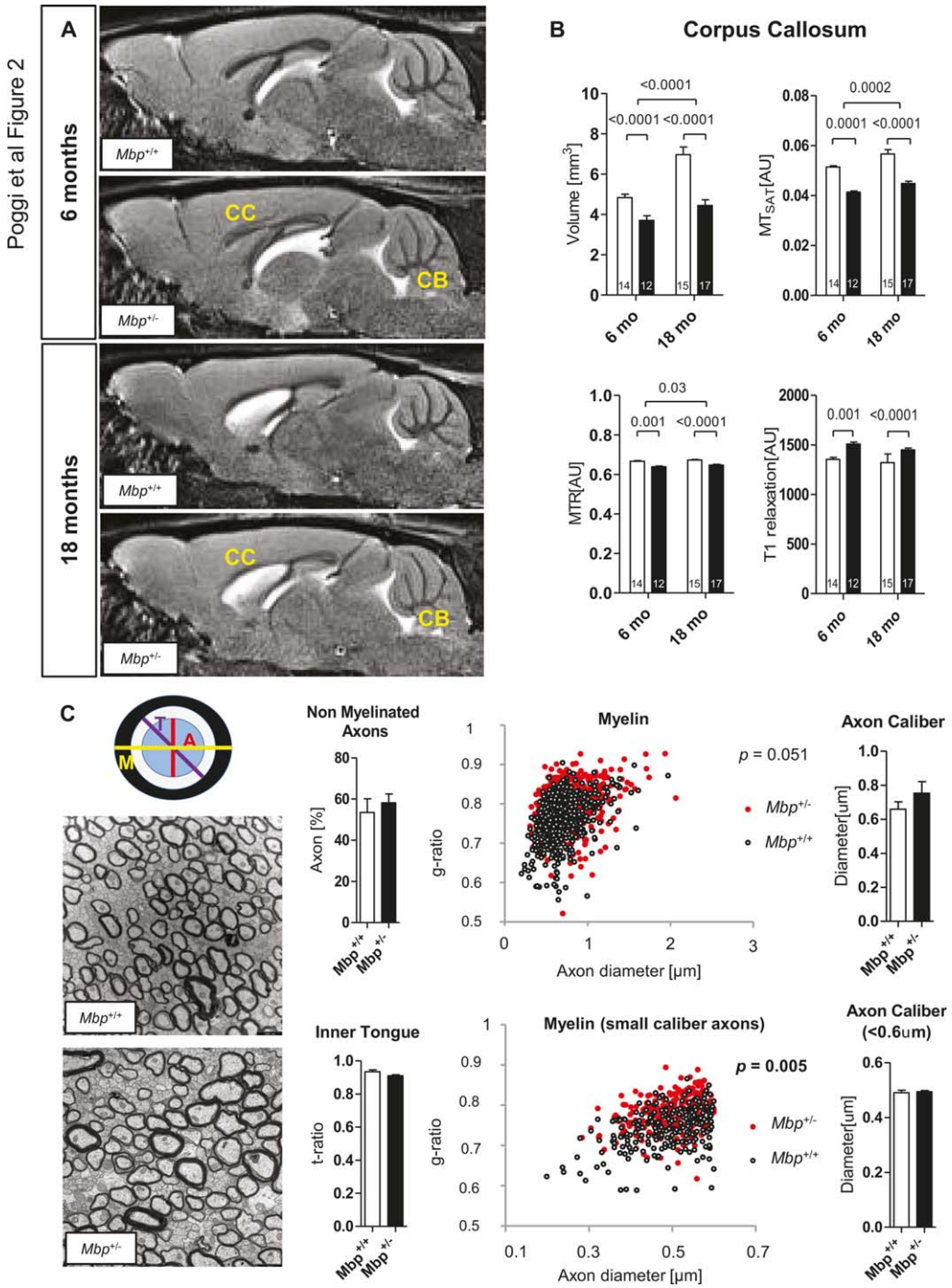

FIGURE 2: Hypomyelination phenotype in the corpus callosum detected by magnetic resonance imaging (MRI) and electron microscopy (EM). A: Sagittal MRI pictures illustrating subtle white matter reduction in CC (corpus callosum) and CB (cerebellum) of *Mbp*$^{+/-}$ versus *Mbp*$^{+/+}$ mice. B: Quantification of corpus callosum MRI data of 6 and 18 months old *Mbp*$^{+/-}$ versus *Mbp*$^{+/+}$, mice demonstrating reduction in volume, as well as in MT_{SAT} and MTR, and increase in T1 relaxation, together consistent with a discrete hypomyelination phenotype in *Mbp*$^{+/-}$ versus *Mbp*$^{+/+}$ mice. N numbers are given in the bars; 2-sided t-tests, mean ± SEM presented. C: EM data of 20 month-old mice, showing in *Mbp*$^{+/-}$ mice borderline reduced overall myelin sheath thickness, which reaches significance in small caliber axons. No changes are seen in % of non-myelinated axons, inner tongue size, or mean axon calibers. A = axon diameter; M = myelin + axon diameter; T = inner tongue + axon diameter; t-ratio = A/T; g-ratio = A/A+(M-T); N = 3 per genotype; 2-sided t-tests, mean ± SEM presented.

myelinated axons or inner tongue size did not yield statistically significant differences between *Mbp*$^{+/-}$ and *Mbp*$^{+/+}$ mice. Whereas g-ratio measurements showed just a tendency of overall reduction of myelin sheath thickness in *Mbp*$^{+/-}$ mice, reduced myelin sheath thickness of small caliber axons (<0.6 µm) was significant.

TABLE 1: Brain Volume, Axonal Fiber Structure and White Matter Integrity of $Mbp^{+/-}$ and $Mbp^{+/+}$ Compared by MRI

Indices	Brain area	6 months			18 months			6 months vs. 18 months (*P* values)		
		$Mbp^{+/+}$ ($n = 14$)	$Mbp^{+/-}$ ($n = 12$)	*P* value	$Mbp^{+/+}$ ($n = 15$)	$Mbp^{+/-}$ ($n = 17$)	*P* value	Genotype	Age	Interaction
Volumetry (mm^3)	Ventricles	10.73 ± 0.38	11.76 ± 0.48	0.1	11.96 ± 0.53	12.57 ± 0.65	0.49	0.13	0.44	0.56
	Cerebellum	59.9 ± 0.67	61.02 ± 0.64	0.24	59.16 ± 0.73	57.89 ± 1.03	0.34	0.93	0.03	0.17
	Olfactory Bulb	26.27 ± 0.44	26.76 ± 0.3	0.37	27.48 ± 0.28	27.07 ± 0.16	0.07	0.78	0.07	0.09
	Brainstem	58.8 ± 1.12	52.99 ± 1.77	0.01	62.35 ± 2.35	61.39 ± 2	0.32	0.17	0.002	0.36
	Brain Matter (excluded the previous)	315.2 ± 3.92	314.4 ± 3.1	0.88	323.6 ± 2.5	314.8 ± 3.81	0.07	0.19	0.22	0.26
Fractional Anisotropy	Corpus Callosum	0.34 ± 0.006	0.35 ± 0.004	0.17	0.37 ± 0.008	0.36 ± 0.011	0.7	0.87	0.02	0.17
Radial Diffusivity ($\cdot 10^{-6}$ mm^2/s)		546 ± 6.3	556 ± 1.1	0.07	506 ± 12	516 ± 9.7	0.32	0.11	<0.0001	0.52
Axial Diffusivity ($\cdot 10^{-6}$ mm^2/s)		908 ± 11	963 ± 12	0.03	905 ± 15	897 ± 13	0.71	0.09	0.02	0.03
Apparent Diffusion Coefficient ($\cdot 10^{-6}$ mm^2/s)		667 ± 7	700 ± 11	0.01	639 ± 12.2	619 ± 27	0.7	0.72	0.005	0.15
Magnetization Transfer Ratio	Corpus Callosum	0.67 ± 0.004	0.64 ± 0.003	**0.001**	0.67 ± 0.002	0.65 ± 0.004	**< 0.0001**	**< 0.0001**	0.03	0.9
Magnetization Transfer Saturation		0.05 ± 0.0005	0.04 ± 0.0004	**0.0001**	0.06 ± 0.002	0.04 ± 0.001	**< 0.0001**	**< 0.0001**	0.0002	0.42
T1 Relaxation		1353 ± 21	1509 ± 19	**0.001**	1322 ± 88	1450 ± 18	**< 0.0001**	0.005	0.36	0.78

Bolded *P* values, "survived" multiple testing adjustment via Bonferroni (MT and DTI: 7 parameters evaluated in one brain region).

TABLE 2: Metabolic Alterations in the Brain of $Mbp^{+/-}$ Versus $Mbp^{+/+}$ Mice Measured by 1H-MRS

Metabolite (mM)	Brain area	6 months			18 months			6 months vs. 18 months (*P* values)		
		$Mbp^{+/+}$ ($n = 14$)	$Mbp^{+/-}$ ($n = 12$)	*P* value	$Mbp^{+/+}$ ($n = 15$)	$Mbp^{+/-}$ ($n = 17$)	*P* value	Genotype	Age	Interaction
Myo-inositol	Cortex	3.49 ± 0.12	3.62 ± 0.1	0.44	3.25 ± 0.12	3.59 ± 0.1	0.02	0.05	0.24	0.36
	Corpus Callosum	3.65 ± 0.06	3.77 ± 0.08	0.09	3.71 ± 0.11	4.15 ± 0.14	0.01	0.016	0.06	0.16
	Hippocampus	4.67 ± 0.16	4.62 ± 0.22	0.85	4.63 ± 0.17	5.04 ± 0.23	0.1	0.38	0.36	0.26
Taurine	Cortex	10.54 ± 0.21	11.17 ± 0.34	0.17	9.21 ± 0.35	10.48 ± 0.22	0.006	**0.001**	**0.0008**	0.27
	Corpus Callosum	10.18 ± 0.16	9.848 ± 0.2	0.3	9.71 ± 0.22	10.46 ± 0.15	0.007	0.26	0.7	0.004
	Hippocampus	11.18 ± 0.22	11.62 ± 0.35	0.28	11.6 ± 0.24	12.02 ± 0.36	0.45	0.17	0.19	0.98
Choline	Cortex	1.24 ± 0.04	1.4 ± 0.13	0.34	1.2 ± 0.05	1.2 ± 0.04	0.49	0.14	0.14	0.34
	Corpus Callosum	1.2 ± 0.02	1.19 ± 0.03	0.74	1.31 ± 0.06	1.32 ± 0.05	0.87	0.99	0.02	0.79
	Hippocampus	1.14 ± 0.04	1.2 ± 0.03	0.21	1.19 ± 0.07	1.22 ± 0.06	0.98	0.42	0.53	0.75
tCreatine	Cortex	7.03 ± 0.16	7.44 ± 0.25	0.45	6.83 ± 0.22	7.55 ± 0.08	**0.002**	0.003	0.82	0.39
	Corpus Callosum	7.72 ± 0.1	7.66 ± 0.11	0.77	8.07 ± 0.11	8.4 ± 0.08	0.02	0.21	**< 0.0001**	0.06
	Hippocampus	8.2 ± 0.12	8.33 ± 0.17	0.53	8.57 ± 0.29	8.96 ± 0.21	0.06	0.24	0.025	0.56
tNAA	Cortex	8.22 ± 0.18	8.62 ± 0.14	0.1	8.27 ± 0.3	8.69 ± 0.12	0.6	0.05	0.76	0.95
	Corpus Callosum	8.06 ± 0.12	7.9 ± 0.11	0.48	7.99 ± 0.12	8.21 ± 0.11	0.19	0.66	0.41	0.16
	Hippocampus	7.5 ± 0.1	7.39 ± 0.17	0.55	7.64 ± 0.14	7.87 ± 0.2	0.62	0.73	0.07	0.3

Bolded *P* values "survived" testing adjustment via Bonferroni (10 comparisons: 5 metabolites and 2 time points per brain region).

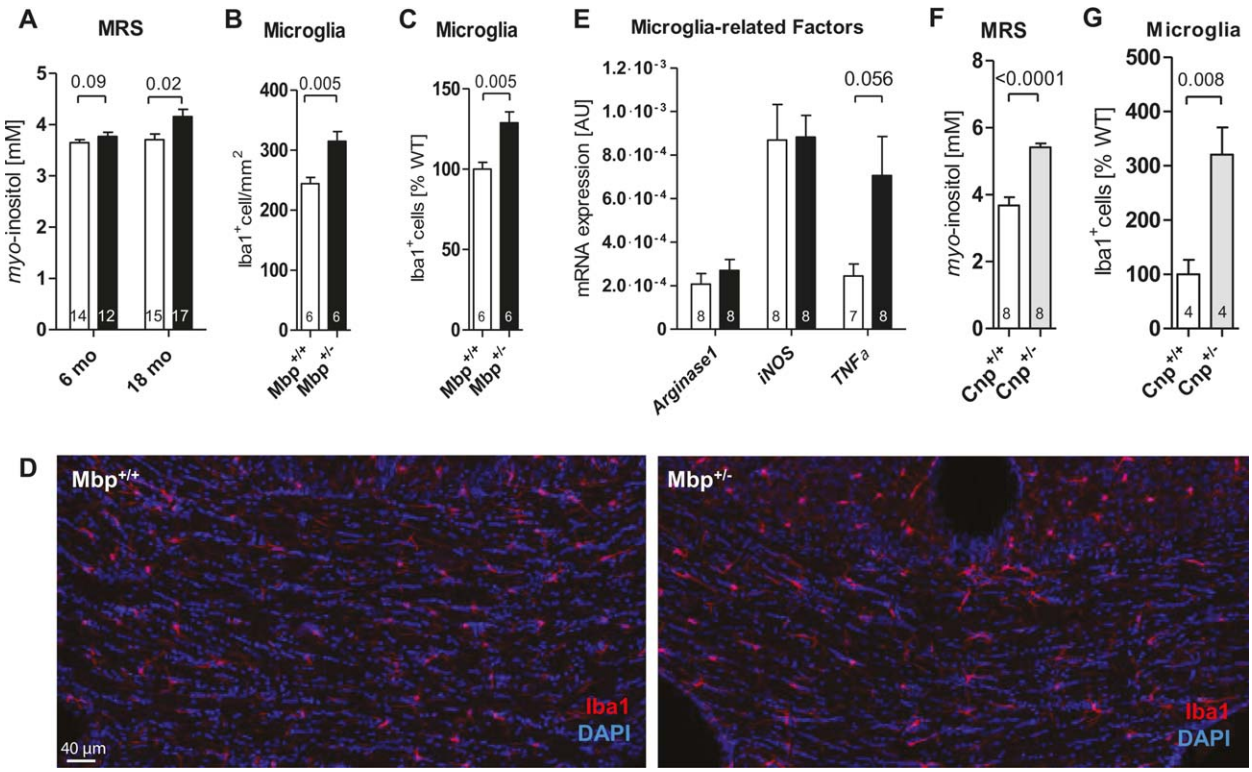

FIGURE 3: Low-grade inflammatory phenotype in the PFC/frontal corpus callosum of *Mbp*$^{+/-}$ mice revealed by magnetic resonance spectroscopy (MRS), microglia counts and TNF-alpha mRNA. A: *Myo*-inositol enhancement in *Mbp*$^{+/-}$ mice, prominent upon aging; B, C: Iba1+ cell increase in 14 month-old *Mbp*$^{+/-}$ mice; D: Representative section scanned for Iba1+ cell counting; E: Elevated TNF-alpha mRNA expression in 18 month-old *Mbp*$^{+/-}$ versus *Mbp*$^{+/+}$ mice. N numbers given in the bars; 2-sided t-tests, mean ± SEM presented. F-G: Single myelin gene-dose reductions *(Mbp, Cnp)* can result in strikingly similar low-grade inflammation phenotypes: Note the highly comparable findings in aging *Cnp*$^{+/-}$ mice: Increase in *myo*-inositol (MRS), and in Iba1+ cells in the frontal corpus callosum. N numbers given in the bars; 2-sided t-tests, mean ± SEM presented.[TQ3]

Microglial Cells in the Corpus Callosum

Since elevated *myo*-inositol has been associated with microgliosis (Badar-Goffer et al., 1992; Ross et al., 1997), we immunostained brain sections of 14-month-old mice for Iba1, a microglia/macrophage-specific cytosolic protein. When quantified in rostral corpus callosum, an approximately 30% increase in Iba1+ cells was found in *Mbp*$^{+/-}$ compared to *Mbp*$^{+/+}$ mice. Notably, there was no obvious change of microglial morphology from the ramified appearance. Activation of microglia/macrophages is supported by a 2-fold increase in TNF-alpha mRNA in PFC of *Mbp*$^{+/-}$ (Fig. 3A–E). A similar picture of low-grade inflammation, including *myo*-inositol increase and microgliosis as shown here for *Mbp*$^{+/-}$ mice, was found in 18 month-old *Cnp*$^{+/-}$ mice (Fig. 3F–G and (Hagemeyer et al., 2012)). We note that in aging *Mbp*$^{+/-}$ mice, Cnp was reduced by 50% in the PFC (see above).

Behavioral Consequences of a Subtle Hypomyelination Phenotype

To clarify whether the subtle hypomyelination phenotype found in *Mbp*$^{+/-}$ mice is by itself the cause of behavioral abnormalities in absence of overt neurological deficits, several cohorts of male mice underwent comprehensive behavioral testing. As listed in Table 3, *Mbp*$^{+/-}$ mice showed normal sensory and motor functions as well as anxiety-like behavior, tested in elevated plus maze and open field. There were no signs of anhedonia, compulsive or abnormal home-cage behavior. Sociability and learning abilities were similar between genotypes. However, *Mbp*$^{+/-}$ mice showed persistent impairment in PPI (Fig. 4A,B). PPI deficit is among the most reliable objective features of severe psychiatric diseases and as such one of the most relevant translational phenotypes (Braff et al., 1978; Fendt and Koch 2013; Kumari et al., 2005). The herewith documented network dysfunction likely affects the ability to adequately filter and interpret environmental stimuli, a common trait in psychiatric disorders. Another network function, the plain startle response, a measure of cerebellar reflex circuitry, tended to be lower in *Mbp*$^{+/-}$ mice at 3 months, and was reduced at 17 months (Fig. 4C). Importantly, *Mbp*$^{+/-}$ mice exhibited upon aging (>16 months) an increasingly catatonic phenotype (Fig. 4D,E, Supp. Info. videos), reminiscent of that described earlier in aged *Cnp*$^{+/-}$ mice (Hagemeyer et al., 2012). Together, our behavioral data

TABLE 3: Behavioral Phenotyping of Male $Mbp^{+/-}$ Versus $Mbp^{+/+}$ Mice at 3 and 17 Months of Age

Behavioral paradigms	3 months					17 months				
	$Mbp^{+/+}$ (*n*)	$Mbp^{+/-}$ (*n*)	$Mbp^{+/+}$	$Mbp^{+/-}$	*P* value	$Mbp^{+/+}$ (*n*)	$Mbp^{+/-}$ (*n*)	$Mbp^{+/+}$	$Mbp^{+/-}$	*P* value
Anxiety and activity										
Elevated plus maze (time close arm [s])	22	34	176 ± 9	166 ± 10	0.67					
Elevated plus maze (time open arm [s])	22	34	31 ± 5	31.28 ± 5	0.79					
Elevated plus maze (time centre [s])	22	34	75 ± 8	78 ± 5	0.67					
Elevated plus maze (total distance [m])	22	34	10.1 ± 0.3	9.46 ± 0.51	0.6					
Elevated plus maze (average speed [mm/s])	22	34	31.8 ± 1.5	33.8 ± 1.2	0.31					
Open field (total distance [m])	22	34	48 ± 1.6	47.6 ± 1.4	0.72	22	33	36.43 ± 1.4	37.2 ± 1.5	0.83
Open field (average velocity [mm/s])	22	34	116.2 ± 3.4	115.3 ± 3.4	0.6	22	33	87.32 ± 3.4	89.13 ± 3.7	0.87
Open field (periphery [s])	22	34	341 ± 9	341 ± 7	0.77	22	33	377 ± 6	374 ± 5	0.92
Open field (intermediate [s])	22	34	60 ± 7	60 ± 5	0.71	22	33	33 ± 4	34 ± 4	0.81
Open field (centre [s])	22	34	19 ± 2	19 ± 2	0.9	22	33	9 ± 2	11 ± 2	0.62
Open field (latency to the periphery [s])	22	34	16 ± 4	15 ± 2	0.21	22	33	27 ± 9	30 ± 6	0.34
Exploratory behavior										
Hole board (holes visited [n])	22	34	5 ± 1	6 ± 1	0.38					
Impulsivity										
Marble burying (marble buried [n])	22	34	7.23 ± 1.14	7.1 ± 0.92	0.9					
Motor learning and coordination										
Rota-rod day 1 (latency to fall [s])	22	34	123 ±15	140 ± 17	0.87	22	33	81 ± 15	96 ± 10	0.23
Rota-rod day 2 (latency to fall [s])	22	34	214 ± 18	208 ± 15	0.79					
Muscle strength										
Grip strength [p]	22	34	142 ± 3	139 ± 2	0.41					
Heat/pain perception										
Hot plate (latency to lick [s])	22	34	15 ± 1	16 ± 1	0.15					
Sight										
Visual cliff (latency in the “air” [%])	22	34	36 ± 4	34 ± 3	0.57	22	33	35 ± 4	26 ± 4	0.11
Olfaction										
Buried food test (digging latency [s])	22	34	87 ± 21	74 ± 13	0.88					

TABLE 3: Continued

Behavioral paradigms	3 months					17 months				
	Mbp$^{+/+}$ (*n*)	*Mbp*$^{+/-}$ (*n*)	*Mbp*$^{+/+}$	*Mbp*$^{+/-}$	*P* value	*Mbp*$^{+/+}$ (*n*)	*Mbp*$^{+/-}$ (*n*)	*Mbp*$^{+/+}$	*Mbp*$^{+/-}$	*P* value
Hearing										
Hearing (startle amplitude [AU])	22	34			Genotype $p = 0.6$ dB p <0.0001	12	16			Genotype $p = 0.505$ dB p>0.0001
Anhedonia										
Sucrose preference test [%]	22	34	74 ± 2	74 ± 2	0.89					
Homecage behavior										
LABORAS (climbing [s])						10	16	2188 ± 429	2480 ± 419	0.64
LABORAS (grooming [s])						10	16	5363 ± 463	4899 ± 457	0.5
LABORAS (locomotion [s])						10	16	2734 ± 295	2859 ± 374	0.85
LABORAS (drinking [s])						10	16	84.5 ± 23	260 ± 56	0.12
LABORAS (eating [s])						10	16	2468 ± 362	2486 ± 272	0.85
LABORAS (scratching [s])						10	16	1065 ± 120	869 ± 217	0.73
LABORAS (circular movements [s])						10	16	541.5 ± 59.2	711.9 ± 107.1	0.51
Sociability										
Three-chambered social test (sociability [%])	22	34	62 ± 2	63 ± 2	0.81			-	-	-
Learning and memory						22	33			
Morris water maze, training (escape latency [s])	22	34			Genotype $p = 0.63$ Time p <0.0001					Genotype $p = 0.69$ Time p<0.0001
Probe trial - time in target zone [%]	22	34	41 ± 2	45 ± 2	0.17	22	33	47 ± 2	54 ± 2	0.09
Escaping latency - reversal [s]	22	34			Genotype $p = 0.28$ Day p<0.0001	22	33			Genotype $p = 0.17$ Day p<0.0001
Probe trial reversal - time in target zone [%]	22	34	33 ± 2	32.7 ± 2	0.54	22	33	41 ± 2	43 ± 2	0.3
Novel object recognition (novelty preference [%])	22	34	59 ± 3	58 ± 3	0.81					
Y-maze (alternation index [#])	22	34	0.7 ± 0.05	0.8 ± 0.03	0.63					

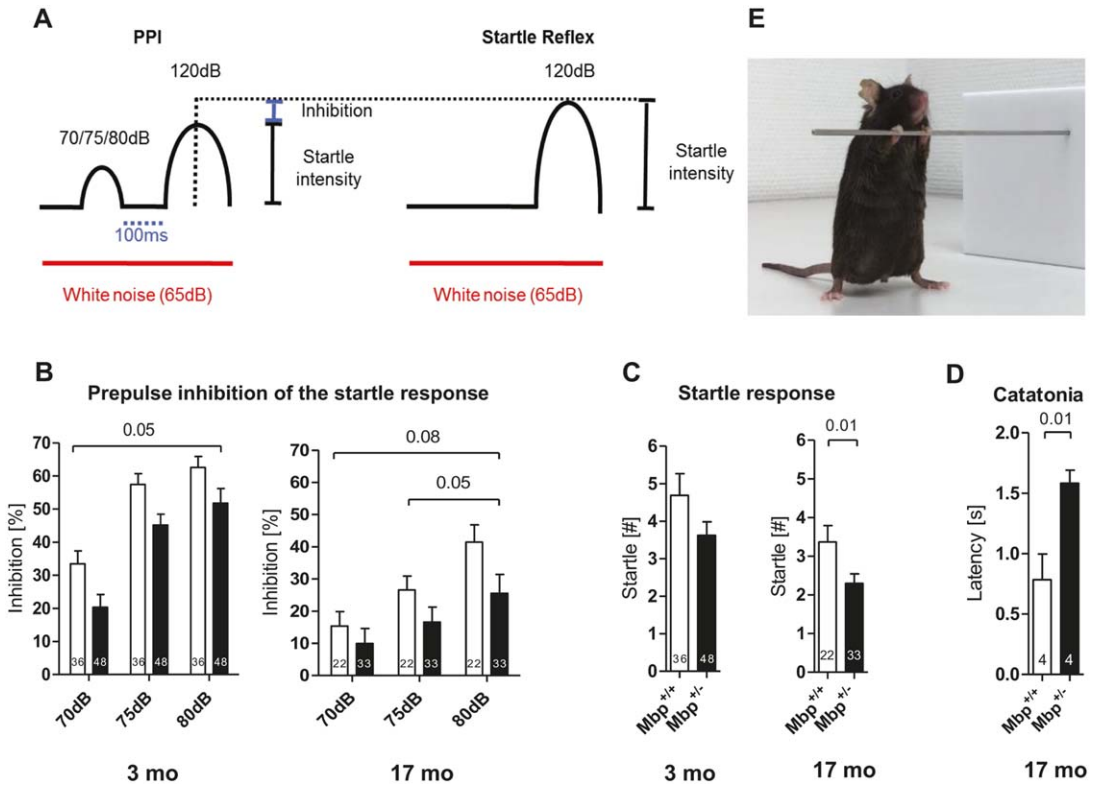

FIGURE 4: Behavioral abnormalities of *Mbp*$^{+/-}$ mice reveal a mental disease-relevant phenotype. A: Prepulse inhibition of the startle response (PPI), experimental design. B: PPI and C: startle response reduction in *Mbp*$^{+/-}$ mice. D: Catatonia in old *Mbp*$^{+/-}$ mice, quantification of time (latency) on the bar; E: Illustrating photograph with typical catatonic posture. N numbers given in the bars; 2-sided t-tests, mean ± SEM presented.

demonstrate that the isolated *Mbp*/Mbp reduction of *Mbp*$^{+/-}$ mice is sufficient to induce measurable network dysfunction in both PFC (PPI) and brainstem (startle), as well as age-related catatonia (frontal corpus callosum), all mental disease-typical features.

Discussion

In human patients with psychiatric diseases, numerous MRI and post-mortem findings have been published that point to subtle white matter abnormalities and myelin loss (Balevich et al., 2015; Chambers and Perrone-Bizzozero, 2004; Dracheva et al., 2006; Flynn et al., 2003; Hakak et al., 2001; Honer et al., 1999; Kochunov et al., 2013; Kubicki et al., 2005; Kubicki et al., 2002; Matthews et al., 2012; McIntosh et al., 2008; Parlapani et al., 2009; Tkachev et al., 2003). However, once complex diseases such as schizophrenia become clinically manifest it is virtually impossible to distinguish cause and consequence of correlative findings. While minor defects of subcortical myelination are unlikely the sole cause of a complex psychiatric disorder, the failure to adequately myelinate cortical fibers is an obvious risk factor for long-range connectivity and may play a causal role when combined with other genetic and environmental risk factors or aging (Nave and Ehrenreich, 2014). On the other hand, clinical and autopsy findings of white matter loss could be merely secondary effects in a long-lasting disease process that primarily perturbs the neuronal circuitry. Myelination defects could finally be secondary after years of pharmacological treatment (Bartzokis et al., 2007; Ho et al., 2011). All these scenarios are not strictly alternative and might act in combination. Mechanistic insight into any of these key variables requires well-defined experimental animal models.

In the present study we addressed the potentially primary role of minor myelination defects for behavior and brain network function. We comprehensively reanalyzed the phenotype of "healthy" *Mbp* heterozygous *Shiverer* mice, a classical line of natural mouse mutants, in which only *Mbp* homozygous mice are dysmyelinated and exhibit severe neurological defects (Chernoff, 1981). Contrary to the early literature with its focus on the homozygous phenotype, we found that central myelination of *Mbp* heterozygous mice is not identical to wildtype controls. Upon gross histological analysis, and when judged by cage-behavior, *Mbp*$^{+/-}$ mice cannot be distinguished from *Mbp*$^{+/+}$ littermates. However, the detailed analysis at biochemical, histological, electron microscopic, MRI/MRS, and behavioral level, revealed intriguing differences. This includes a mild hypomyelination of the PFC, with signs of microglial activation, combined with prepulse inhibition

(PPI) deficits and clinical signs of catatonia upon aging in the presence of otherwise normal behavioral performance.

The principle finding (by histology and MRI) is a subtle hypomyelination of the PFC of adult mice and a thinning of the underlying corpus callosum, i.e., regions relevant for cognitive functions and catatonia. Oligodendrocytes were probably not diminished in number, as suggested by unaltered mRNA abundance of myelin protein genes (except for *Mbp* itself), indicating that hypomyelination is unlikely caused by a paucity of mature oligodendrocytes.

Our attempt to confirm the histologically documented hypomyelination by EM as a reduction of myelin sheath thickness yielded only borderline significance, except for small caliber fibers which had a larger g-ratio. This supports an alternative working model, in which myelination by *Mbp* heterozygous oligodendrocytes is less efficient at an early stage of ensheathment. For example, a small fraction of oligodendroglial processes might normally contact axons and initiate myelination, but then fail to continue wrapping and instead retract, which would lead to a reduced number of myelinated internodes. This model is compatible with current concepts of CNS myelination and the role of activity-dependent *Mbp* mRNA translation at the tip of an oligodendrocyte process (Wake et al., 2011). Here, Mbp is essential in stabilizing the first membrane wraps that have been deposited in order for myelination to proceed (Simons and Nave, 2016; Snaidero et al., 2014). We further note that in wild type mice, axons of cortical projection neurons are often incompletely myelinated along their length (Tomassy et al., 2014). This suggests that myelination signals in the cortex are indeed weak in comparison to other CNS regions, such as spinal cord or optic nerve, where virtually all axons are fully myelinated at late postnatal stages. We therefore propose that translating 50% *Mbp* mRNA (in $Mbp^{+/-}$ mice) may be sufficient for oligodendrocytes in the spinal cord, which are exposed to strong axonal signals, to stabilize the initial wraps and robustly myelinate axons. Thus, in *Mbp* heterozygous oligodendrocytes of the PFC myelination may be inefficient because here axonal signals, including their spiking activity, are weak compared e.g. to the spinal cord. Such a working model is clearly speculative, but fully compatible with experimental observations in other labs (Lundgaard et al., 2013; Tomassy et al., 2014; Wake et al., 2011). It could explain why at higher age the amount of Mbp in the PFC of heterozygotes has dropped below the expected 50%. This differs from the brainstem, where axonal activity is less likely to decrease with age and where myelination remains robust. Our data also match prior experiments in wild type mice, which have shown that reduced social activity during postnatal development has a negative impact on myelination, specifically of the PFC and its underlying white matter (Liu et al., 2012; Makinodan et al., 2012). Collectively, these *in vivo* observations support the idea that cortical myelination is stimulated by neuronal activity, and that the strength of this signal differs between CNS regions and presumably at different stages of life.

By 1H-MRS, we detected elevated *myo*-inositol levels in white matter that corresponded to the histologically determined increase in microglial cells and elevated TNF-alpha expression. We have no evidence for underlying axonal degeneration in white matter tracts, or that low-grade microglial activation is a response to the assembly of unstable myelin, as by electron microscopy compact myelin appears fully stable with only 50% Mbp incorporated. Interestingly, neuroinflammation in white matter tracts is a major feature of mice homozygous and heterozygous null for the *Cnp* gene (Hagemeyer et al., 2012; Lappe-Siefke et al., 2003), and we measured at the protein level a 50% reduction of Cnp (but not Plp) in the cortex of aged $Mbp^{+/-}$ mice. Cnp is a structural protein of non-compacted myelin that antagonizes MBP during myelin compaction by maintaining "myelinic channels" open (Snaidero et al., 2014). The mechanism of reduced Cnp/CNP in cortical white matter of $Mbp^{+/-}$ mice or in autopsy material from patients with schizophrenia (Dracheva et al., 2006; Flynn et al., 2003; Hakak et al., 2001; Prabakaran et al., 2004) is unknown. However, it is plausible that loss of Cnp/CNP-dependent metabolic support for myelinated axons triggers (unknown) stress signals that activate resident microglial cells. Above threshold or upon "secondary hits," as shown for *Cnp* heterozygous mice (Wieser et al., 2013), neuroinflammation in white matter tracts can also drive axonal degeneration, which generates a vicious circle of events that is relevant for neuropsychiatric diseases.

At the behavioural level, $Mbp^{+/-}$ mice are still below threshold of a clear psychiatric disease phenotype, as evidenced by a comprehensive battery of tests, in which they exhibit normal basic behavior and higher brain functions including cognition. However, already at age 3 months they showed deficits of sensorimotor gating with reduced PPI, a physiological phenomenon shared between human patients with schizophrenia and rodent disease models (Swerdlow et al., 2008). The link between *Mbp* heterozygosity and PPI deficits is unclear, but is likely reflecting subtle myelin abnormalities and desynchronized impulse propagation. We note that also *Plp1* overexpressing mice share mild PPI deficits, but in the presence of other schizophrenia-relevant defects (Tanaka et al., 2009). Another network disturbance (i.e. of a cerebellar reflex circuitry) of $Mbp^{+/-}$ mice is indicated by the here observed reduction in the startle response. Interestingly, a similar phenomenon has been reported in a mouse model of chronic stress (Dirks et al., 2002). Most importantly, later in life, $Mbp^{+/-}$ mice exhibit a catatonia-like behavior that we have previously seen in $Cnp^{+/-}$ mice upon aging (Hagemeyer

et al., 2012), suggesting again that reduced Cnp expression and mild neuroinflammation, downstream of a slightly abnormal CNS myelin assembly, may predispose to this schizophrenia-relevant frontal cortical phenotype.

In summary, the reduction of *Mbp*/Mbp induces subtle hypomyelination, accompanied by low-grade inflammation, leading to cortical network dysfunction. This reveals that *Mbp*/Mbp decrease per se can be causative of psychiatric illness-relevant phenotypes.

Acknowledgment

Grant sponsor: Max Planck Society, DFG Research Center for Nanoscale Microscopy and Molecular Physiology of the Brain (CNMPB), EXTRABRAIN EU-FP7.

Author Contributions

Concept and design of the study: HE, KAN

Data acquisition and analysis: GP, SB, WM, TR, JB, NM, GW, IH, SG, HW

Drafting the manuscript and display items: HE, KAN, GP

All authors read and approved the final version of the manuscript.

References

Badar-Goffer RS, Ben-Yoseph O, Bachelard HS, Morris PG. 1992. Neuronal-glial metabolism under depolarizing conditions. A 13C-n.m.r. study. Biochem J 282:225–230.

Balevich EC, Haznedar MM, Wang E, Newmark RE, Bloom R, Schneiderman JS, Aronowitz J, Tang CY, Chu KW, Byne W, Buchsbaum MS, Hazlett EA. 2015. Corpus callosum size and diffusion tensor anisotropy in adolescents and adults with schizophrenia. Psychiatry Res 231:244–251.

Barbarese E, Nielson ML, Carson JH. 1983. The effect of the shiverer mutation on myelin basic protein expression in homozygous and heterozygous mouse brain. J Neurochem 40:1680–1686.

Bartzokis G, Lu PH, Nuechterlein KH, Gitlin M, Doi C, Edwards N, Lieu C, Altshuler LL, Mintz J. 2007. Differential effects of typical and atypical antipsychotics on brain myelination in schizophrenia. Schizophr Res 93:13–22.

Benes FM. 1989. Myelination of cortical-hippocampal relays during late adolescence. Schizophr Bull 15:585–593.

Bodda C, Tantra M, Mollajew R, Arunachalam JP, Laccone FA, Can K, Rosenberger A, Mironov SL, Ehrenreich H, Mannan AU. 2013. Mild overexpression of Mecp2 in mice causes a higher susceptibility toward seizures. Am J Pathol 183:195–210.

Braff D, Stone C, Callaway E, Geyer M, Glick I, Bali L. 1978. Prestimulus effects on human startle reflex in normals and schizophrenics. Psychophysiology 15:339–343.

Bu J, Banki A, Wu Q, Nishiyama A. 2004. Increased NG2(+) glial cell proliferation and oligodendrocyte generation in the hypomyelinating mutant shiverer. Glia 48:51–63.

Catani M, ffytche DH. 2005. The rises and falls of disconnection syndromes. Brain 128:2224–2239.

Chambers JS, Perrone-Bizzozero NI. 2004. Altered myelination of the hippocampal formation in Subjects with schizophrenia and bipolar disorder. Neurochem Res 29:2293–2302.

Chernoff GF. 1981. Shiverer: an autosomal recessive mutant mouse with myelin deficiency. J Hered 72:128

Dere E, Dahm L, Lu D, Hammerschmidt K, Ju A, Tantra M, Kästner A, Chowdhury K, Ehrenreich H. 2014. Heterozygous Ambra1 deficiency in mice: A genetic trait with autism-like behavior restricted to the female gender. Front Behav Neurosci 8:181

Dirks A, Groenink L, Schipholt MI, van der Gugten J, Hijzen TH, Geyer MA, Olivier B. 2002. Reduced startle reactivity and plasticity in transgenic mice overexpressing corticotropin-releasing hormone. Biol Psychiatry 51:583–590.

Dracheva S, Davis KL, Chin B, Woo DA, Schmeidler J, Haroutunian V. 2006. Myelin-associated mRNA and protein expression deficits in the anterior cingulate cortex and hippocampus in elderly schizophrenia patients. Neurobiol Dis 21:531–540.

El-Kordi A, Winkler D, Hammerschmidt K, Kästner A, Krueger D, Ronnenberg A, Ritter C, Jatho J, Radyushkin K, Bourgeron T, Fischer J, Brose N, Ehrenreich H. 2013. Development of an autism severity score for mice using Nlgn4 null mutants as a construct-valid model of heritable monogenic autism. Behav Brain Res 251:41–49.

El Idrissi A, Trenkner E. 1999. Growth factors and taurine protect against excitotoxicity by stabilizing calcium homeostasis and energy metabolism. J Neurosci 19:9459–9468.

Feinstein A, Magalhaes S, Richard JF, Audet B, Moore C. 2014. The link between multiple sclerosis and depression. Nat Rev Neurol 10:507–517.

Fendt M, Koch M. 2013. Translational value of startle modulations. Cell Tissue Res 354:287–295.

Fields RD, Araque A, Johansen-Berg H, Lim SS, Lynch G, Nave KA, Nedergaard M, Perez R, Sejnowski T, Wake H. 2014. Glial biology in learning and cognition. Neuroscientist 20:426–431.

Flynn SW, Lang DJ, Mackay AL, Goghari V, Vavasour IM, Whittall KP, Smith GN, Arango V, Mann JJ, Dwork AJ, Falkai P, Honer WG. 2003. Abnormalities of myelination in schizophrenia detected in vivo with MRI, and post-mortem with analysis of oligodendrocyte proteins. Mol Psychiatry 8:811–820.

Gibson EM, Purger D, Mount CW, Goldstein AK, Lin GL, Wood LS, Inema I, Miller SE, Bieri G, Zuchero JB, Barres BA, Woo PJ, Vogel H, Monje M. 2014. Neuronal activity promotes oligodendrogenesis and adaptive myelination in the mammalian brain. Science 344:480–481.

Hagemeyer N, Goebbels S, Papiol S, Kästner A, Hofer S, Begemann M, Gerwig UC, Boretius S, Wieser GL, Ronnenberg A, Gurvich A, Heckers SH, Frahm J, Nave K-A, Ehrenreich H. 2012. A myelin gene causative of a catatonia-depression syndrome upon aging. EMBO Mol Med 4:528–539.

Hakak Y, Walker JR, Li C, Wong WH, Davis KL, Buxbaum JD, Haroutunian V, Fienberg AA. 2001. Genome-wide expression analysis reveals dysregulation of myelination-related genes in chronic schizophrenia. Proc Natl Acad Sci USA 98:4746–4751.

Henkelman RM, Stanisz GJ, Graham SJ. 2001. Magnetization transfer in MRI: A review. NMR Biomed 14:57–64.

Ho BC, Andreasen NC, Ziebell S, Pierson R, Magnotta V. 2011. Long-term antipsychotic treatment and brain volumes: A longitudinal study of first-episode schizophrenia. Arch Gen Psychiatry 68:128–137.

Honer WG, Falkai P, Chen C, Arango V, Mann JJ, Dwork AJ. 1999. Synaptic and plasticity-associated proteins in anterior frontal cortex in severe mental illness. Neuroscience 91:1247–1255.

Hyde TM, Ziegler JC, Weinberger DR. 1992. Psychiatric disturbances in metachromatic leukodystrophy: Insights into the neurobiology of psychosis. Arch Neurol 49:401–406.

Jahn O, Tenzer S, Werner HB. 2009. Myelin proteomics: Molecular anatomy of an insulating sheath. Mol Neurobiol 40:55–72.

Jung M, Sommer I, Schachner M, Nave KA. 1996. Monoclonal antibody O10 defines a conformationally sensitive cell-surface epitope of proteolipid protein (PLP): Evidence that PLP misfolding underlies dysmyelination in mutant mice. J Neurosci 16:7920–7929.

Kim YS, Harry GJ, Kang HS, Goulding D, Wine RN, Kissling GE, Liao G, Jetten AM. 2010. Altered cerebellar development in nuclear receptor TAK1/TR4 null mice is associated with deficits in GLAST(+) glia, alterations in social behavior, motor learning, startle reactivity, and microglia. Cerebellum 9:310–323.

Klugmann M, Schwab MH, Puhlhofer A, Schneider A, Zimmermann F, Griffiths IR, Nave KA. 1997. Assembly of CNS myelin in the absence of proteolipid protein. Neuron 18:59–70.

Kochunov P, Glahn DC, Rowland LM, Olvera RL, Winkler A, Yang YH, Sampath H, Carpenter WT, Duggirala R, Curran J, Blangero J, Hong LE. 2013. Testing the hypothesis of accelerated cerebral white matter aging in schizophrenia and major depression. Biol Psychiatry 73:482–491.

Kubicki M, Park H, Westin CF, Nestor PG, Mulkern RV, Maier SE, Niznikiewicz M, Connor EE, Levitt JJ, Frumin M, Kikinis R, Jolesz FA, McCarley RW, Shenton ME. 2005. DTI and MTR abnormalities in schizophrenia: Analysis of white matter integrity. NeuroImage 26:1109–1118.

Kubicki M, Westin C-F, Maier SE, Frumin M, Nestor PG, Salisbury DF, Kikinis R, Jolesz FA, McCarley RW, Shenton ME. 2002. Uncinate fasciculus findings in schizophrenia: A magnetic resonance diffusion tensor imaging study. Am J Psychiatry 159:813–820.

Kumari V, Das M, Zachariah E, Ettinger U, Sharma T. 2005. Reduced prepulse inhibition in unaffected siblings of schizophrenia patients. Psychophysiology 42:588–594.

Kuschinsky K, Hornykiewicz O. 1972. Morphine catalepsy in the rat: Relation to striatal dopamine metabolism. Eur J Pharmacol 19:119–122.

Lappe-Siefke C, Goebbels S, Gravel M, Nicksch E, Lee J, Braun PE, Griffiths IR, Nave KA. 2003. Disruption of Cnp1 uncouples oligodendroglial functions in axonal support and myelination. Nat Genet 33:366–374.

Liu J, Dietz K, DeLoyht JM, Pedre X, Kelkar D, Kaur J, Vialou V, Lobo MK, Dietz DM, Nestler EJ, Dupree J, Casaccia P. 2012. Impaired adult myelination in the prefrontal cortex of socially isolated mice. Nat Neurosci 15:1621–1623.

Lowry OH, Rosebrough NJ, Farr AL, Randall RJ. 1951. Protein measurement with the Folin phenol reagent. J Biol Chem 193:265–275.

Lundgaard I, Luzhynskaya A, Stockley JH, Wang Z, Evans KA, Swire M, Volbracht K, Gautier HOB, Franklin RJM, ffrench-Constant C, Attwell D, Káradóttir RT. 2013. Neuregulin and BDNF induce a switch to NMDA receptor-dependent myelination by oligodendrocytes. PLoS Biol 11:e1001743.

Makinodan M, Rosen KM, Ito S, Corfas G. 2012. A critical period for social experience-dependent oligodendrocyte maturation and myelination. Science 337:1357–1360.

Matthews PR, Eastwood SL, Harrison PJ. 2012. Reduced myelin basic protein and actin-related gene expression in visual cortex in schizophrenia. PLoS ONE 7:e38211

McIntosh AM, Munoz Maniega S, Lymer GK, McKirdy J, Hall J, Sussmann JE, Bastin ME, Clayden JD, Johnstone EC, Lawrie SM. 2008. White matter tractography in bipolar disorder and schizophrenia. Biol Psychiatry 64:1088–1092.

Miller DJ, Duka T, Stimpson CD, Schapiro SJ, Baze WB, McArthur MJ, Fobbs AJ, Sousa AM, Sestan N, Wildman DE, Lipovich L, Kuzawa CW, Hof PR, Sherwood CC. 2012. Prolonged myelination in human neocortical evolution. Proc Natl Acad Sci USA 109:16480–16485.

Moy SS, Nadler JJ, Perez A, Barbaro RP, Johns JM, Magnuson TR, Piven J, Crawley JN. 2004. Sociability and preference for social novelty in five inbred strains: An approach to assess autistic-like behavior in mice. Genes Brain Behav 3:287–302.

Nave KA. 2010. Myelination and support of axonal integrity by glia. Nature 468:244–252.

Nave KA, Ehrenreich H. 2014. Myelination and oligodendrocyte functions in psychiatric diseases. JAMA Psychiatry 71:582–584.

Parlapani E, Schmitt A, Erdmann A, Bernstein HG, Breunig B, Gruber O, Petroianu G, von Wilmsdorff M, Schneider-Axmann T, Honer W, Falkai P. 2009. Association between myelin basic protein expression and left entorhinal cortex pre-alpha cell layer disorganization in schizophrenia. Brain Res 1301:126–134.

Prabakaran S, Swatton JE, Ryan MM, Huffaker SJ, Huang JT, Griffin JL, Wayland M, Freeman T, Dudbridge F, Lilley KS, Karp NA, Hester S, Tkachev D, Mimmack ML, Yolken RH, Webster MJ, Torrey EF, Bahn S. 2004. Mitochondrial dysfunction in schizophrenia: Evidence for compromised brain metabolism and oxidative stress. Mol Psychiatry 9:684–697. 643-

Provencher SW. 1993. Estimation of metabolite concentrations from localized in vivo proton NMR spectra. Magn Reson Med 30:672–679.

Radyushkin K, El-Kordi A, Boretius S, Castaneda S, Ronnenberg A, Reim K, Bickeböller H, Frahm J, Brose N, Ehrenreich H. 2010. Complexin2 null mutation requires a 'second hit' for induction of phenotypic changes relevant to schizophrenia. Genes Brain Behav 9:592–602.

Readhead C, Popko B, Takahashi N, David Shine H, Saavedra RA, Sidman RL, Hood L. 1987. Expression of a myelin basic protein gene in transgenic shiverer mice: Correction of the dysmyelinating phenotype. Cell 48:703–712.

Roach A, Takahashi N, Pravtcheva D, Ruddle F, Hood L. 1985. Chromosomal mapping of mouse myelin basic protein gene and structure and transcription of the partially deleted gene in shiverer mutant mice. Cell 42:149–155.

Rosenbluth J. 1980. Peripheral myelin in the mouse mutant Shiverer. J Comp Neurol 193:729–739.

Ross BD, Bluml S, Cowan R, Danielsen E, Farrow N, Gruetter R. 1997. In vivo magnetic resonance spectroscopy of human brain: The biophysical basis of dementia. Biophys Chem 68:161–172.

Schmahmann JD, Smith EE, Eichler FS, Filley CM. 2008. Cerebral white matter: neuroanatomy, clinical neurology, and neurobehavioral correlates. Ann NY Acad Sci 1142:266–309.

Shine HD, Readhead C, Popko B, Hood L, Sidman RL. 1992. Morphometric analysis of normal, mutant, and transgenic CNS: Correlation of myelin basic protein expression to myelinogenesis. J Neurochem 58:342–349.

Simons M, Nave KA. 2016. Oligodendrocytes: Myelination and axonal support. Cold Spring Harb Perspect Biol 8:a020479

Snaidero N, Mobius W, Czopka T, Hekking LH, Mathisen C, Verkleij D, Goebbels S, Edgar J, Merkler D, Lyons DA, Nave KA, Simons M. 2014. Myelin membrane wrapping of CNS axons by PI(3,4,5)P3-dependent polarized growth at the inner tongue. Cell 156:277–290.

Swerdlow NR, Weber M, Qu Y, Light GA, Braff DL. 2008. Realistic expectations of prepulse inhibition in translational models for schizophrenia research. Psychopharmacology 199:331–388.

Takahashi N, Sakurai T, Davis KL, Buxbaum JD. 2011. Linking oligodendrocyte and myelin dysfunction to neurocircuitry abnormalities in schizophrenia. Prog Neurobiol 93:13–24.

Takeuchi T, Kiyama Y, Nakamura K, Tsujita M, Matsuda I, Mori H, Munemoto Y, Kuriyama H, Natsume R, Sakimura K, Mishina M. 2001. Roles of the glutamate receptor epsilon2 and delta2 subunits in the potentiation and prepulse inhibition of the acoustic startle reflex. Eur J Neurosci 14:153–160.

Tanaka H, Ma J, Tanaka KF, Takao K, Komada M, Tanda K, Suzuki A, Ishibashi T, Baba H, Isa T, Shigemoto R, Ono K, Miyakawa T, Ikenaka K. 2009. Mice with altered myelin proteolipid protein gene expression display cognitive deficits accompanied by abnormal neuron-glia interactions and decreased conduction velocities. J Neurosci 29:8363–8371.

Tkachev D, Mimmack ML, Ryan MM, Wayland M, Freeman T, Jones PB, Starkey M, Webster MJ, Yolken RH, Bahn S. 2003. Oligodendrocyte dysfunction in schizophrenia and bipolar disorder. Lancet 362:798–805.

Tomassy GS, Berger DR, Chen HH, Kasthuri N, Hayworth KJ, Vercelli A, Seung HS, Lichtman JW, Arlotta P. 2014. Distinct profiles of myelin distribution along single axons of pyramidal neurons in the neocortex. Science 344: 319–324.

Uda S, Matsui M, Tanaka C, Uematsu A, Miura K, Kawana I, Noguchi K. 2015. Normal development of human brain white matter from infancy to early adulthood: A diffusion tensor imaging study. Dev Neurosci 37:182–194.

Uhlhaas Peter J, Singer W. 2012. Neuronal dynamics and neuropsychiatric disorders: Toward a translational paradigm for dysfunctional large-scale networks. Neuron 75:963–980.

Uranova NA, Vikhreva OV, Rachmanova VI, Orlovskaya DD. 2011. Ultrastructural alterations of myelinated fibers and oligodendrocytes in the prefrontal cortex in schizophrenia: A postmortem morphometric study. Schizophr Res Treatment 2011:325789

Uranova NA, Vostrikov VM, Orlovskaya DD, Rachmanova VI. 2004. Oligodendroglial density in the prefrontal cortex in schizophrenia and mood disorders: A study from the Stanley Neuropathology Consortium. Schizophr Res 67:269–275.

Urenjak J, Williams SR, Gadian DG, Noble M. 1993. Proton nuclear magnetic resonance spectroscopy unambiguously identifies different neural cell types. J Neurosci 13:981–989.

Wake H, Lee PR, Fields RD. 2011. Control of local protein synthesis and initial events in myelination by action potentials. Science 333: 1647–1651.

Wieser GL, Gerwig UC, Adamcio B, Barrette B, Nave KA, Ehrenreich H, Goebbels S. 2013. Neuroinflammation in white matter tracts of Cnp1 mutant mice amplified by a minor brain injury. Glia 61:869–880.

Zatorre RJ, Fields RD, Johansen-Berg H. 2012. Plasticity in gray and white: Neuroimaging changes in brain structure during learning. Nat Neurosci 15: 528–536.

Zhang R, He J, Zhu S, Zhang H, Wang H, Adilijiang A, Kong L, Wang J, Kong J, Tan Q, Li X-M. 2012. Myelination deficit in a phencyclidine-induced neurodevelopmental model of schizophrenia. Brain Res 1469:136–143.